

Thermal inversion analysis in the Andorran Central Valley and its relationship with pollutants and meteorological variables

Author: Alex Crespillo López

University Supervisor: Mireia Udina i Sistach, mudina@meteo.ub.edu (1)

External Supervisor: Laura Trapero Bagué, ltrapero@ari.ad (2)

(1) Facultat de Física, University of Barcelona, Diagonal 645, 08028 Barcelona, Spain.

(2) Andorra Recerca + Innovació. Av. Rocafort 21-23 building Molí 3rd floor, AD600 Sant Julià de Lòria, Andorra.*

Abstract: The interplay between the boundary layer and orography in mountainous regions creates complex atmospheric dynamics influencing pollutant behavior, particularly noticeable in winter due to prevalent thermal inversion episodes. This study aims to characterise these episodes in the Andorran Central Valley, assessing their average characteristics and correlation with pollutant and meteorological variables. Additionally, the efficacy and accuracy of low-cost sensors of temperature, in contrast to official surface stations, are evaluated for temperature measurements. Findings indicate an increasing frequency and duration of thermal inversion episodes over the years, predominantly influenced by synoptic high-pressure conditions. These episodes significantly affect NO₂ concentrations, nearly doubling their average levels, while PM₁₀ and O₃ show no direct correlation. Furthermore, the effectiveness of low-cost sensors is notably dependent on their placement, particularly in terms of altitude and orientation relative to solar radiation.

I. INTRODUCTION

Air quality and pollution present significant challenges in areas with complex orography, where the movement and dispersion of airborne particles are limited by the landscape and local meteorological phenomena (*Giovannini et al. (2020)*). This leads to hazardous conditions impacting humans, flora, fauna, and even construction materials. In mountainous regions, such as the Andorran Central Valley, persistent thermal inversions, which inhibit atmospheric dispersion, are primary contributors to severe air quality issues.

Among the primary pollutants of concern are nitrogen dioxide (NO₂), particulate matter (PM₁₀), and ozone (O₃). NO₂ often originates from traffic emissions and industrial activities, significantly impacting air quality, especially in urbanized valleys (*De Wekker et al. (2018)*). PM₁₀ particles, which include dust, pollen, and soot, can be attributed to both natural sources, such as Saharan dust intrusions, and anthropogenic sources like vehicle emissions and industrial processes. Ozone, a secondary pollutant, forms through complex photochemical reactions involving primary pollutants like NO_x and volatile organic compounds (VOCs) in the presence of sunlight (*Grau and Cuxart (2020)*). Its concentration relies on the equilibrium between formation and depletion reactions, involving NO_x in both cases.

Thermal inversion episodes are more prevalent in winter when synoptic anticyclonic conditions predominate. These conditions create a calm atmosphere with a low isobaric gradient, leading to minimal or absent wind situations. The formation of a stable layer near the surface can trap pollutants, exacerbating air quality issues (*Pepin and Kidd (2006)*).

To accurately assess thermal inversions, various methods are employed, each with its unique strengths and limitations. Radiosondes, which are weather balloons equipped with sensor packages, provide valuable data by measuring atmospheric conditions as they ascend through the air column. They offer detailed vertical profiles of temperature, humidity, and wind, crucial for identifying and analyzing thermal inversions (*Fochesatto (2015)*).

Ground-based stations at different altitudes are also instrumental in monitoring thermal inversions. By comparing temperature and other meteorological data between lower and higher altitude stations, it's possible to identify the presence and intensity of thermal inversions (*Fochesatto (2015)*). For instance, a higher temperature reading at an elevated station compared to one at a lower altitude can be indicative of an inversion scenario. This is the method employed in this work.

Furthermore, computational models are extensively used to simulate and predict thermal inversions. However, their effectiveness is often constrained by resolution limitations, especially in complex terrains like mountainous regions. Most models are optimized for flat terrains and may not accurately capture the nuances of atmospheric processes in areas with variable topography (*Pageès and Miró (2017)*). This highlights the importance of integrating diverse measurement methods to gain a comprehensive understanding of thermal inversion phenomena.

In recent years, the advent of low-cost sensors has introduced a new dimension to environmental monitoring, particularly in the study of air quality and meteorological phenomena like thermal inversions. These sensors offer a cost-effective alternative to traditional monitoring equipment, enabling broader spatial coverage and the possibility of deploying sensor networks in areas where conventional stations are not feasible. While they may

* Electronic address: acresplo8@alumnes.ub.edu

not match the precision of standard meteorological equipment, low-cost sensors are increasingly recognized for their utility in providing valuable data, especially when calibrated and used in conjunction with traditional measurement methods.

Their application in monitoring thermal inversions is particularly promising. By strategically placing these sensors at various altitudes and locations within a complex terrain like the Andorran Central Valley (Fig 2), it's possible to gather a more nuanced understanding of thermal inversion dynamics. This approach can complement the data obtained from higher-cost stations and models, offering a more comprehensive view of the inversion phenomena and its impact on air quality.

The current study aims to address these challenges by focusing on the Andorran Central Valley, a region prone to thermal inversions and associated air quality issues (*Govern d'Andorra* (2017)). The first part of the research will analyze thermal inversion events from 2005 to September 2023 only using 2 traditional stations, correlating them with meteorological and pollutant data. The second part will evaluate the efficacy of low-cost sensors alongside the traditional method of using stations at different altitudes, determining their reliability in capturing the dynamics of thermal inversions in complex terrains like the Andorran Central Valley. In addition, the combined results from the service stations and low-cost sensors will be tested for its reliability to obtain conclusions.

II. DATA AND METHODOLOGY

The analyses and visualizations presented in this master's thesis were conducted using Python, leveraging a suite of specialized libraries to facilitate data processing and graphical representation. Specifically, the libraries utilized include Pandas for data manipulation and analysis, Matplotlib and Seaborn for data visualization, NumPy for numerical computations, Calendar for handling dates and times, and Wind Rose for representing wind speed and direction data. These tools were instrumental in extracting insights and generating the plots and results showcased in this thesis.

A. Study Area

Andorra, a small mountainous country of 468 km², is nestled in the Eastern Pyrenees, bordered by the autonomous community of Catalonia (Spain) to the south and France to the north. With an average elevation of 1996 meters above sea level (ASL), it stands as the highest country in Europe and one of the most elevated globally. The topography of Andorra features three narrow valleys forming a Y shape, with secondary valleys extending perpendicular to this primary structure. The focal area of this study is the point where these three main valleys converge, creating a relatively flat terrain known

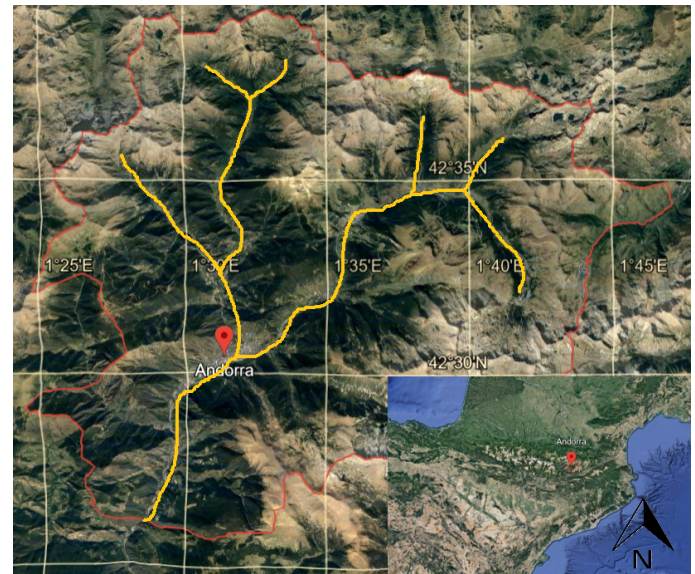


Figure 1: Top view of Andorra and its administrative boundaries with geographical coordinates. Source: Google Earth

as the Andorran Central Valley (Fig 1). This valley hosts the majority of the nation's activities and population, including the capital, Andorra la Vella.

The Andorran Central Valley encompasses an area of approximately 3 km² and a perimeter of 15 km, as determined using Google Earth 2023. It is encircled by peaks reaching nearly 2400 meters along its lateral margins. The valley floor itself lies at an elevation of about 950 to 1050 meters and is oriented from southwest to northeast (Google Earth 2023) (Fig 1).

Owing to its orography and morphology, the valley has emerged as the country's hub, attracting significant industrial and civil activity. As a narrow and relatively confined valley, it tends to trap cold, dense air, making thermal inversion episodes frequent. These inversions, compounded by pollution from various sources (predominantly NO_x emissions from traffic hotspots), can lead to severe health hazards (*Govern d'Andorra* (2020)).

B. Observational data

Observational data for this study were obtained from various stations situated along the Andorran Central Valley. The primary stations, Prat Gran and Engolasters, are represented in red in Fig 2. Prat Gran, positioned at an altitude of 1080 meters, is located in the urbanized central area of the valley, whereas Engolasters, at 1638 meters, is situated in a more vegetated area near a lake. Both stations monitor the same meteorological variables, including wind speed and direction at 2 meters, temperature at 2 meters, relative humidity at 2 meters, precipitation, and incident shortwave radiation. They also measure pollutant concentrations, encompassing NO₂, PM₁₀,

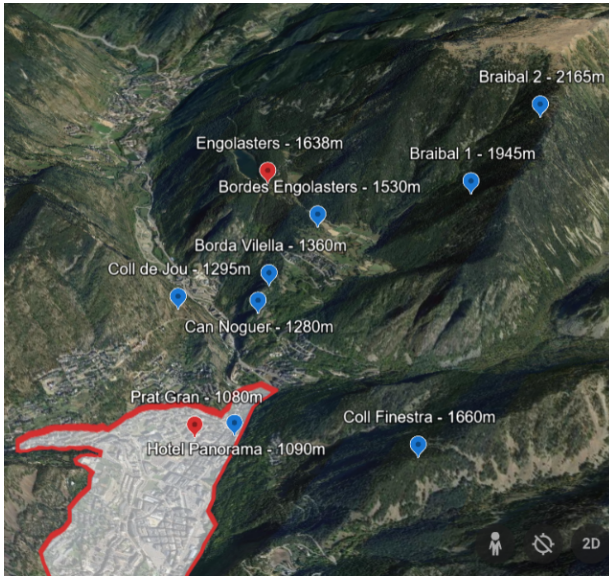


Figure 2: Andorran Central Valley with all the station's locations with their respective altitudes.

Source: Google Earth

PM_{2.5}, SO₂, CO, and NO at Prat Gran, and O₃ at Engolasters.

The meteorological data spans from January 2005 to September 2023, recorded at 15-minute intervals, while pollution concentration data extends from January 2005 to December 2022, documented with an hourly temporal resolution. These stations are managed by the Air Quality Department of the Andorra Government.

Additionally, eight low-cost sensors, known as tiny tags and depicted in blue in Fig 2, are dispersed at various locations and altitudes within the area of study. These sensors exclusively record meteorological variables: temperature at 2 meters, minimum temperature at 2 meters, precipitation, and dew point temperature at 2 meters. The data from these sensors covers the period from January 2020 to November 2023. However, not all sensors provide a complete dataset, as some were installed at different times. Each sensor records data with an hourly temporal resolution and is operated by 'Andorra Recerca + Innovació'.

C. Data Quality Control

Ensuring the reliability of data is paramount for establishing a robust database. Consequently, the collected data underwent a rigorous cleaning and modification process using Python programming to assure its quality. Initially, a statistical analysis was conducted to identify which sensors required cleaning. The primary challenge encountered in the dataset was the presence of missing values, attributed to various causes, such as inadequate maintenance during the COVID-19 pandemic. Additionally, minor issues like measurement errors and

outliers were rectified. This was achieved by comparing the data with historical records and assigning reasonable values, while carefully considering the occurrence of extreme events.

A significant task involved reconciling the time frequency discrepancies between the 15-minute interval data from the Air Quality Department (specifically from Prat Gran and Engolasters stations) and the hourly data from the tiny tags. A harmonization process was implemented to align these datasets to a consistent hourly frequency. This integration resulted in a comprehensive dataset encompassing 10 stations, spanning from 2020 to September 2023 (table A.1). It should be noted that data prior to 2020 is exclusively available from the Prat Gran and Engolasters stations.

D. Methodology

Initially, the study focused on characterizing thermal inversion episodes over the entire time interval (2005-2023) and analyzing meteorological data and pollutant levels to assess changes in boundary layer features and behaviors over the years. Subsequently, data from the tiny tags were incorporated to deepen the understanding of recent thermal inversion episodes (2020-2023) and to evaluate their efficacy and placement. For the initial part of the study, data exclusively from Prat Gran and Engolasters stations were utilized to estimate the occurrence of thermal inversion episodes in the valley. The temperature difference at 2 meters between these stations was calculated using the following equation (*Beaufils* (2021)):

$$\Delta T = T_{2mE} - T_{2mPG} \quad (1)$$

A positive value of ΔT in Eq. 1 indicates the presence of a thermal inversion episode in the Andorran Central Valley. After applying Equation 1, a significant number of short-lived episodes (lasting less than 1 hour) were identified and analyzed separately. For most results, only thermal inversion periods exceeding 1 hour were considered. Seasonal trends were defined with winter from November to March and summer from April to October.

Following the identification of these episodes, the **Inversion Strength (IST)**, measured in °C/km, was determined using Equation 2 (*Beaufils* (2021)):

$$IST = \frac{1}{n} \sum_{i=1}^n \frac{(T_{2mE} - T_{2mPG})}{(Alt_E - Alt_{PG})} \times 1000 \quad (2)$$

This measure enabled the quantification and analysis of inversion strength and its evolution over time. Subsequently, the relationship between pollutants, meteorological variables, and thermal inversion episodes was examined.

The second part of the study involved incorporating data from the tiny tags sensors, located at various positions (Fig 2). Temperature data from these sensors were

compared with that from the Andorra Government stations for study the thermal inversion events. Integrating this data with that from the Air Quality Department resulted in a database comprising 10 stations at different locations and altitudes (table A.1). Plots representing all defined thermal inversion episodes by Prat Gran and Engolasters since 2020, lasting over 1 hour 338 episodes, were generated, incorporating 2m temperature measurements from the tiny tags. Each plot encompassed a 3-hour interval within every event, with additional plots for 1 hour preceding and following each event to assist in identifying temperature gradient shifts.

Subsequent to plotting and qualitative analysis, station measurements were subjected to statistical analysis using the **Standard deviation equation**:

$$\sigma = \sqrt{\frac{1}{N} \sum_{i=1}^N (x_i - \mu)^2} \quad (3)$$

and the **Mean Absolute Deviation (MAD) equation:**

$$MAD = \frac{1}{N} \sum_{i=1}^N |x_i - \bar{x}| \quad (4)$$

The aim was to ascertain the reliability and utility of each station for future vertical profile plots.

III. RESULTS AND DISCUSSION

This section presents the findings of the research, offering a detailed analysis of the evolution of thermal inversion episodes over the studied time interval. Additionally, it provides insights into the interplay between meteorological factors and pollution levels in relation to these episodes. A comprehensive discussion is included to enhance the understanding of the complex dynamics governing thermal inversions and their environmental impact. The results are not only indicative of historical patterns but also shed light on potential future trends in thermal inversion occurrences and their associated consequences in the context of climatic variations and anthropogenic influences.

A. Thermal Inversion Characterization

The analysis of the processed data reveals a total of 1139 thermal inversion episodes, each lasting more than one hour, from January 2005 to September 2023. Notably, there has been an increasing trend in the frequency of these episodes, with the year 2022 recording the highest number at 108. The majority of these episodes (98%) had durations less than 24 hours, and only 22 episodes

exceeded this duration. As depicted in Fig 3, over 50% of the total inversion episodes fall into the more than 1h to 6h duration category, while the percentage occurrence of episodes decreases with increasing duration.

The data indicates a relatively stable trend in inversion strength throughout the time interval (Fig A.1), maintaining minimal year-to-year variations and an average of 2.29 °C/km. Despite this general stability, occasional outliers are observed, corresponding to episodes with a significant temperature gradient between the valley bottom and the Engolasters station.

Seasonal variation in the occurrence of episodes and their inversion strength is also notable. These are generally lower in the summer months (April-October) and more pronounced during the winter (November-March), correlating with the larger temperature gradient observed in winter (Fig A.2). This pattern can be attributed to warm air advections at altitude in winter months, which produce anomalous temperatures. Such advections tend to raise temperatures at the valley tops and hillsides while leaving colder air at the valley bottom, thereby facilitating thermal inversion. In contrast, during summer, warm air advections also occur, but the absence of cold air in the atmosphere results in a smaller temperature gradient between the stations.

Moreover, the analysis indicates a significant correlation between the inversion strength and the duration of thermal inversion episodes, as illustrated in Fig 4. This correlation suggests that a greater temperature gradient often leads to increased difficulties in disrupting the inversion (*Bergot (1994)*). Daytime solar insolation contributes to the formation of a shallow surface convective layer, which, however, is insufficient to dissipate the more persistent inversion layers, as noted by *Largerion and Staquet (2016)*. The strength of this relationship was quantitatively assessed using the Pearson correlation coefficient, yielding a value of 0.53. This positive correlation coefficient indicates a moderate relationship, implying that as the inversion strength increases, so does the likelihood of longer-duration thermal inversion episodes.

B. Meteorological Analysis

Episode	Duration	Mean Inversion Strength (°C/ km)
29-12-2021	4d 9h 45m	5.93
29-11-2015	3d 20h 45m	5.09
27-12-2016	2d 21h 30m	5.64

Table I: Starting date, duration, and mean inversion strength of the 3 major lasting episodes.

Meteorological data has been instrumental in this study, shedding light on the interaction of thermal inversion episodes with various atmospheric variables, including precipitation, wind direction and speed, and temperature, among others. The behavior of these variables

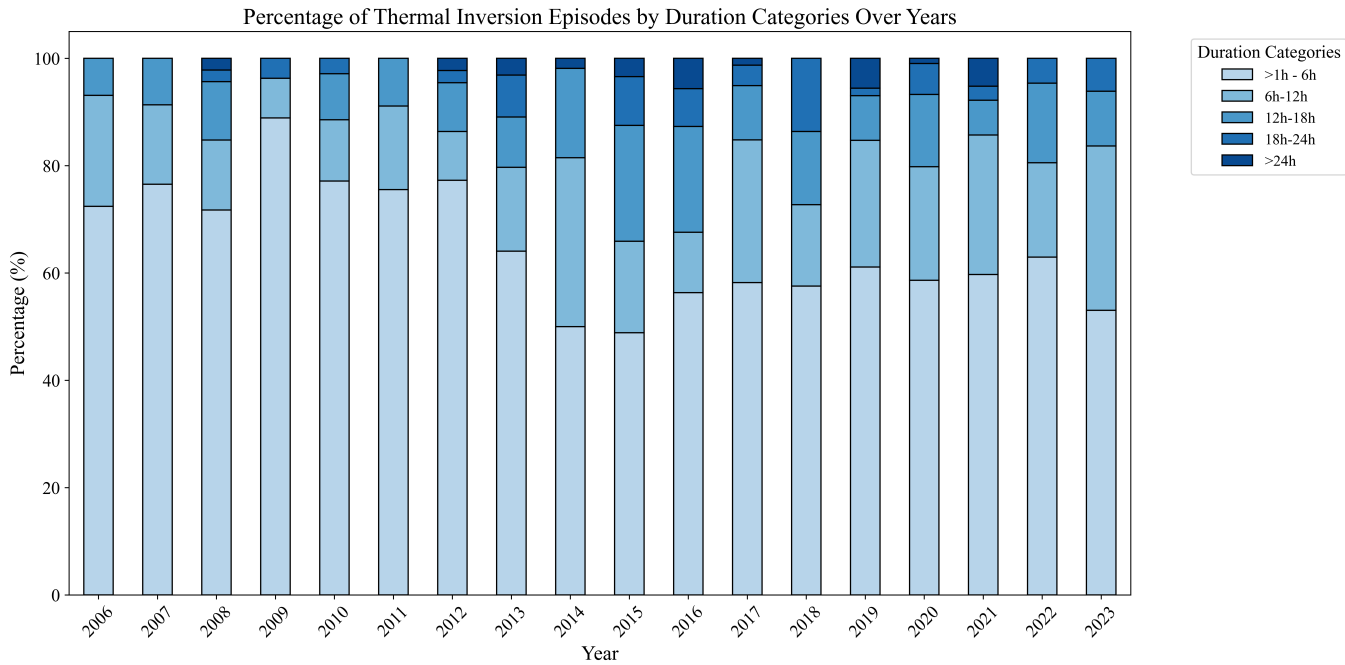


Figure 3: Hourly duration ranges according their % of occurrence over the years. Note that longer episodes have been more common in the recent years.

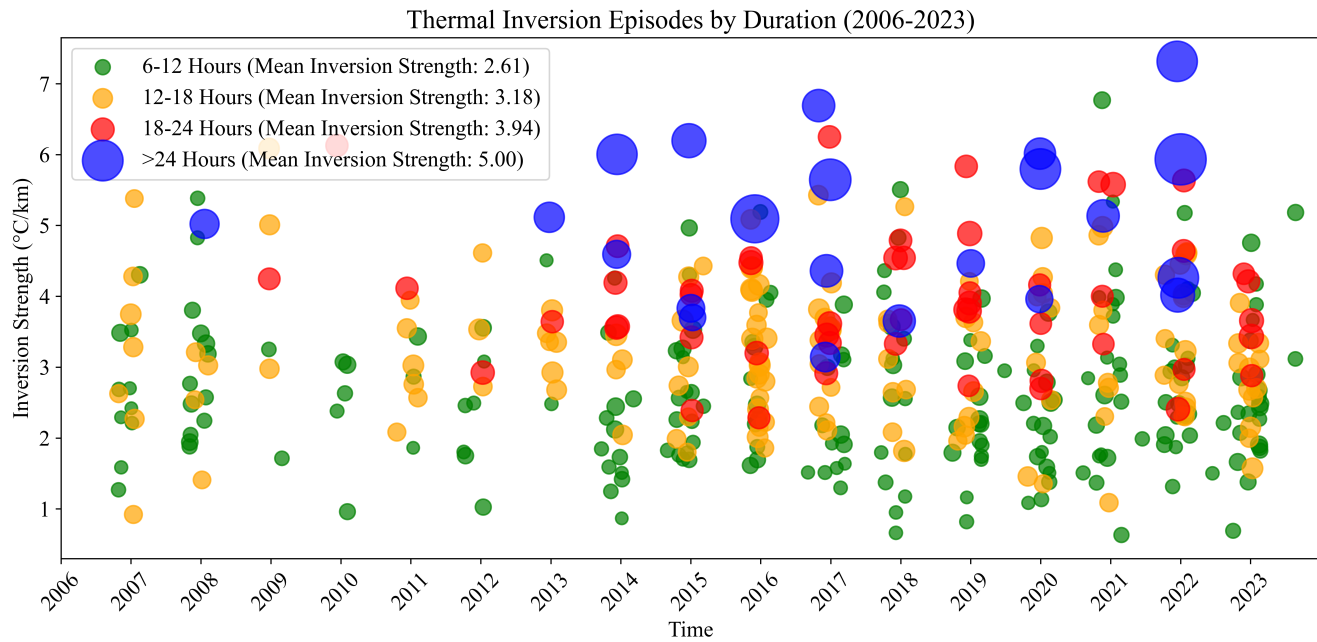


Figure 4: Thermal inversion episodes over the years, displaying their duration with the point size variations. More than 1h up to 6h category was excluded for a better visualisation.

was scrutinised in three specific cases of prolonged thermal inversion episodes (table I).

Concerning temperature, all three events exhibited a consistent pattern, reflecting the diurnal/nocturnal cycle with relatively similar temperature ranges during the

episodes. The temperature variations were generally between 2 to 16°C, although in the longest episode (Fig 5), slightly higher temperatures of 4 to 18°C were observed (Fig 5.a), which are unusually high for the respective month.

Wind direction showed distinct characteristics between locations (Fig 5.b). At Prat Gran station, a consistent northeast direction ($50\text{--}70^\circ$) was observed, influenced by the urban landscape, as the station is situated along a street oriented in this direction, channeling the wind flows. In contrast, Engolasters station exhibited a broader range of wind directions, with a slight dominance of the northeast direction, aligning with the valley's orientation.

Wind speed during the three episodes was notably low at both stations, averaging below 3 m/s, without significant peaks (Fig 5.d). Precipitation was recorded in two out of three episodes, exclusively at Engolasters, and at different times. For the 2016 episode (table I), intermittent light precipitation occurred until mid-episode, whereas in the 2021 episode (Fig 5.c), precipitation marked the end of the event with slightly higher intensity, potentially contributing to the disruption of the stable layer.

These observations suggest that calm conditions, characterized by the absence of precipitation or significant wind, tend to facilitate thermal inversions. Conversely, disturbances such as precipitation or wind can disrupt the stable layer (*Mason (1989)*), leading to the breakdown of the inversion. For both stations, wind direction and speed displayed negative correlations with thermal inversion episodes (positive ΔT) (Fig A.3), as did temperature and precipitation. Similarly, incident solar radiation also showed negative correlations. Relative humidity was the only variable demonstrating a positive correlation with thermal inversion episodes at Prat Gran, while at Engolasters, it correlated negatively.

C. Pollutants Analysis

The evolution of pollutant concentrations in Andorra and their correlation with thermal inversion episodes over the years has been a significant aspect of this study. The Air Quality Department of the Andorra Government reports a notable decline in pollutant levels since 2006, primarily attributed to emissions reduction policies (*Govern d'Andorra (2022)*). Among various pollutants, NO_2 has emerged as the predominant concern.

An examination of the NO_2 concentration distribution (Fig A.4) reveals peaks closely linked to traffic emissions, particularly evident during rush hours and on workdays. The periods of highest NO_2 levels are typically observed between 8:00 – 9:00 and 18:00 – 20:00 (local time). Furthermore, a distinct seasonal trend is apparent, with winter exhibiting higher NO_2 concentrations. This increase can be attributed to heightened anthropogenic activities, such as the use of household heating systems (*Russo et al. (2020)*), and a greater frequency of thermal inversion episodes.

A crucial component of this research involved elucidating the interplay between NO_2 concentration fluctuations and thermal inversion events. The findings indicate that

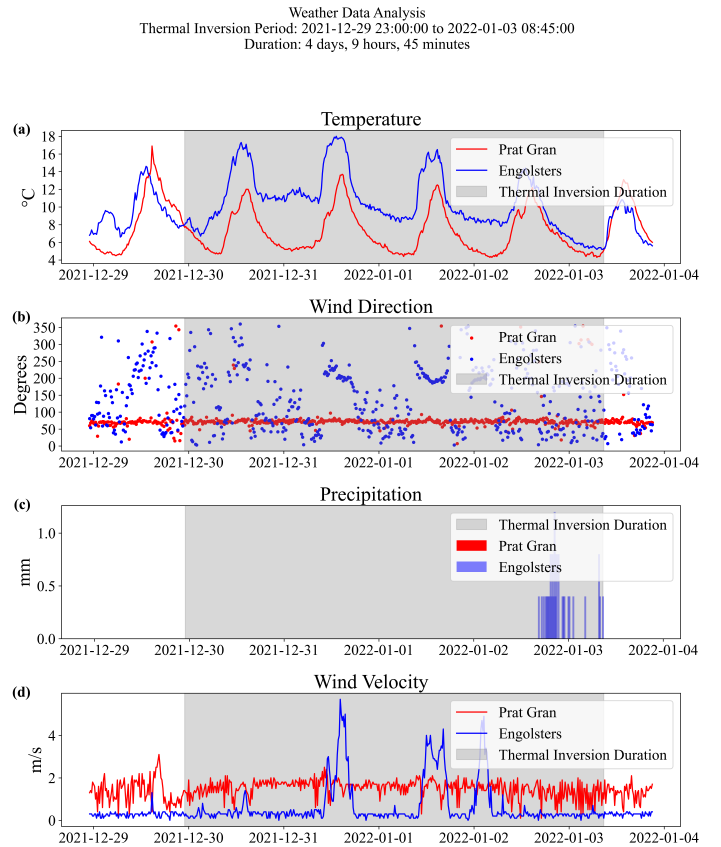


Figure 5: 29-12-2021 episode (longest) meteorological analysis.

thermal inversion episodes significantly contribute to the accumulation of NO_2 . During these events, NO_2 concentrations are observed to be double that of non-inversion periods (Fig 6.c). This phenomenon is primarily due to the formation of a stable atmospheric layer, which hinders both vertical and horizontal dispersion of pollutants. Consequently, NO_2 is closely associated with in-situ formation through chemical reactions. The positive correlation between NO_2 concentrations and thermal inversion episodes is evident in the correlation matrix (Fig A.3).

The daily distribution of PM_{10} particles exhibits a pattern somewhat similar to that of NO_2 , as depicted in Fig 6.a. Peak concentrations are observed during the early morning hours, coinciding with increased anthropogenic activity. However, the daily fluctuations of PM_{10} are not as pronounced as those of NO_2 . A notable contrast emerges when examining the seasonal distribution of PM_{10} , primarily due to its sources. A significant proportion of PM_{10} particles originate from Saharan dust intrusions, which are more prevalent in the summer months (*Russo et al. (2020)*). During thermal inversion episodes, a slight increase in PM_{10} concentration is observed, suggesting a positive correlation (Fig A.3).

In contrast, the behavior of ozone (O_3) markedly dif-

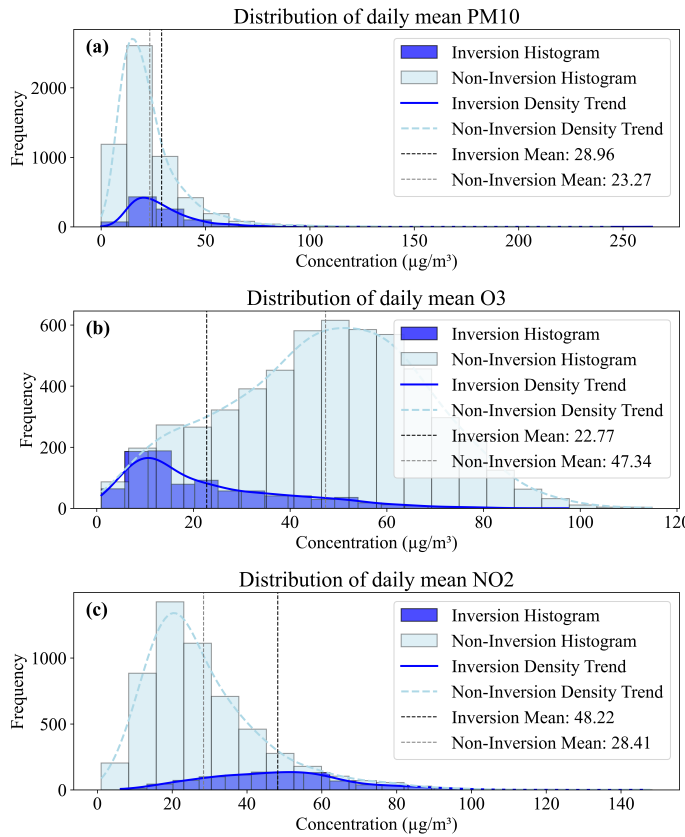


Figure 6: Histograms of PM₁₀ (a), O₃ (b) and NO₂ (c) mean daily concentrations during inversion and non-inversion periods.

fers from that of NO₂ and PM₁₀ due to its unique formation process. Ozone generation requires a photochemical reaction that involves solar radiation. Consequently, the observed data align with this understanding, showing that O₃ levels peak during midday hours (12-16 h) when solar radiation is at its maximum, and are higher in the summer for the same reason. As for the variability of O₃ concentrations during thermal inversion episodes, the findings reveal a substantial decrease in O₃ levels in the presence of these episodes (Fig 6.b). This phenomenon can be largely attributed to the increased levels of NO_x, which act as depletion agents in the formation reactions of ozone (*Lu and Shen (2019)*).

In the context of thermal inversions, none of the pollutants studied (NO₂, PM₁₀, and O₃) exhibited a relationship with inversion strength or the duration of the episodes. This highlights the complex dynamics of air quality during thermal inversion conditions. With respect to meteorological data, NO₂ and PM₁₀ demonstrate a correlation with temperature, indicating their tendency to accumulate during thermal inversion episodes. Conversely, O₃ shows a more pronounced relationship with wind speed and direction, suggesting that it is often transported from more distant sources.

D. Tiny Tags Analysis

Prior to conducting the statistical analysis, a qualitative review of the plots generated for the 338 thermal inversion episodes lasting more than 1 hour since 2020 was undertaken as is detailed in the methodology. This preliminary examination aimed to visually assess the data consistency and identify any apparent discrepancies in the vertical temperature profiles captured by the different stations. Notably, the results from these plots revealed inconsistencies in the vertical profiles (Fig 7), underscoring the need for a more rigorous statistical analysis.

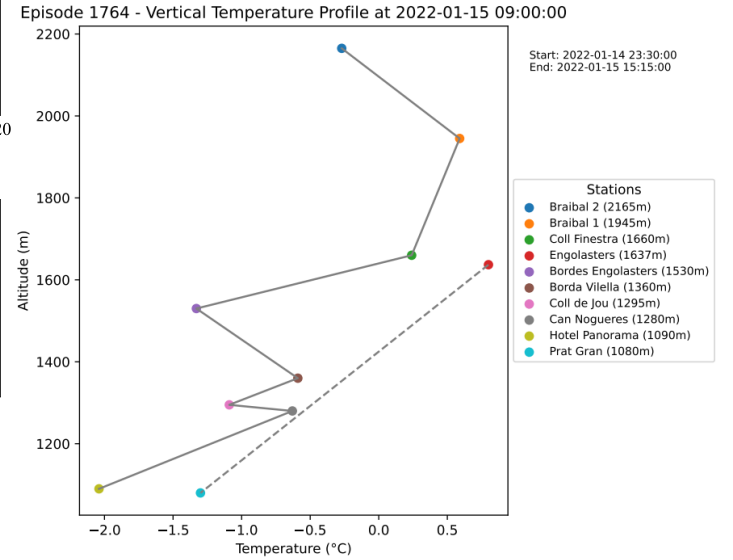


Figure 7: Vertical profiles for an specific episode. Notice the differences between the reference stations (dashed line) and the tiny tags.

The analysis encompasses a comparison of stations based on their proximity, altitude, and corresponding temperature readings. This comparative approach provides insights into the influence of geographical and non-meteorological factors on the observed data. The following subsections detail the specific results for each station comparison.

Prat Gran (1080 m) vs. Hotel Panorama (1090 m): The results indicate that Hotel Panorama has a minimal average temperature difference from Prat Gran, at -0.73°C (Fig 8.e), which is the least among all stations. This minimal difference is consistent with its close proximity and slightly higher altitude compared to Prat Gran. The standard deviation (SD) for Hotel Panorama relative to Prat Gran is notably low, only surpassed by Engolasters. However, when compared to Engolasters, Hotel Panorama's SD is unexpectedly high (table A.2), suggesting other influencing factors.

Braibal 1 (1945 m) and Braibal 2 (2165 m): Both stations exhibit temperature deviations from Prat Gran and Engolasters, with Braibal 2 showing more negative deviations (table A.2) due to its higher altitude. The

SD values relative to Prat Gran are among the highest, indicative of the significant altitude difference. The Mean Absolute Deviation (MAD) values are also the highest for these stations relative to Prat Gran (table A.2). In contrast, their SD values relative to Engolasters are the lowest, yet their MAD values show divergent behavior, with Braibal 1 being lower and Braibal 2 higher (table A.2).

Can Noguer (1280 m), Coll de Jou (1295 m), Borda Vilella (1360 m): These stations, being at similar altitudes, show consistent temperature differences relative to Prat Gran, with more negative values at higher altitudes (Fig 8.b, d and a). Their SD values relative to Prat Gran increase with altitude, while the MAD values show a similar trend among these stations. Compared to Engolasters, the SD values of these stations do not decrease uniformly with altitude, and their MAD values decrease as the altitude approaches that of Engolasters (table A.2).

Bordes Engolasters (1530m), Engolasters (1638m), Coll Finestra (1660 m): The temperature differences from Prat Gran among these stations are intriguing, as they do not become more negative with increasing altitude (Fig 8.f and c). The SD values relative to Prat Gran increase with altitude, with Coll Finestra having the highest value. When compared to Engolasters, Bordes Engolasters SD is unexpectedly high, and Coll Finestra's SD is the highest among all stations, suggesting significant variability (table A.2).

Overall Results: The proximity and altitude play a critical role in the similarity of climatic conditions among the stations, but anomalies suggest the influence of additional factors. The variability, as measured by the Standard Deviation and Mean Absolute Deviation in table A.2, which are basic dispersion measures, shows unexpected patterns, especially in relation to Engolasters, indicating specific local factors or potential inaccuracies in data. Coll Finestra, in particular, exhibits significant variability, warranting further investigation. Non-meteorological factors, such as station location, may be influencing the observed temperature patterns and variability.

Station Name	Altitude (m)	Avg Temp Diff (°C)
Borda Vilella	1360	1.27
Can Nogueres	1280	2.06
Coll Finestra	1660	0.05
Coll de Jou	1295	1.89
Hotel Panorama	1090	2.98
Bordes Engolasters	1530	-0.09
Braibal 1	1945	-1.69
Braibal 2	2165	-2.66

Table II: Average Temperature Differences Using Engolasters (1638m) as Reference. The table contains same numerical information as the Fig 8

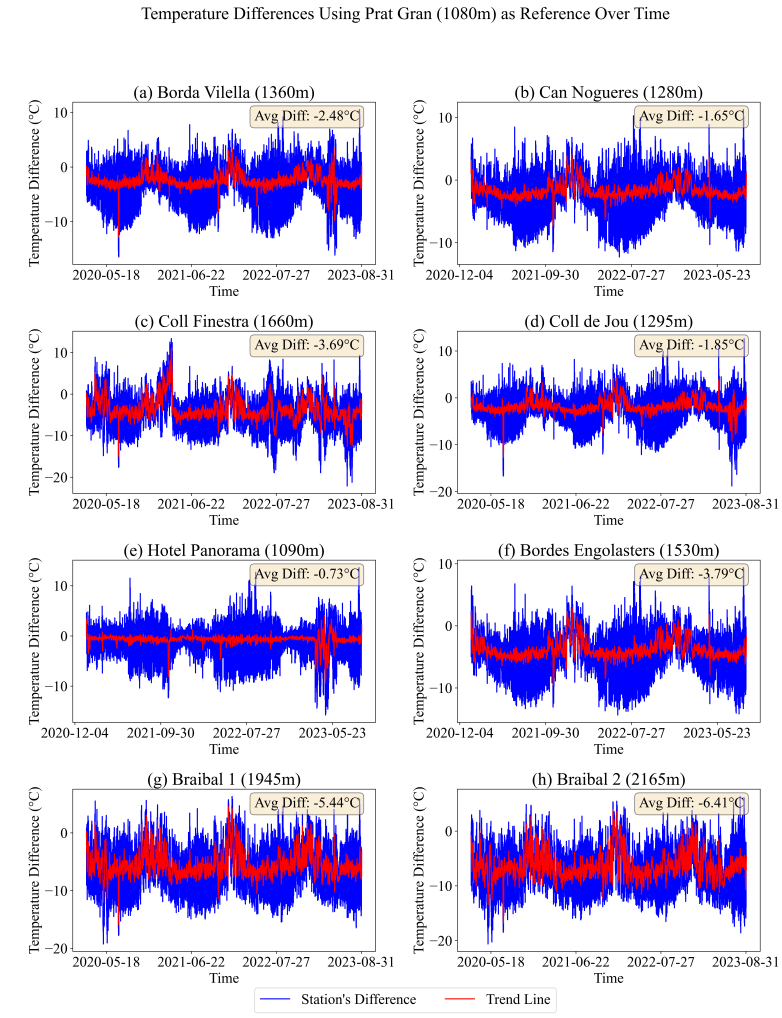


Figure 8: Differences in temperature readings Using Prat Gran (1080m) as reference. Blue color represent the station's difference and red the trend line.

IV. CONCLUSIONS

This research has undertaken a comprehensive analysis of thermal inversion episodes in the Andorran Central Valley from January 2005 to September 2023. The study has provided valuable insights into the dynamics of thermal inversions, their impact on meteorological variables and air quality, and the potential of low-cost sensors in complex orographic terrains.

- Increasing Trend in Thermal Inversions:** A notable increase in the frequency and duration of thermal inversion episodes has been observed, especially during the winter months. While the specific origins of these inversions are complex and multifaceted, involving various atmospheric processes, the study suggests possible contributions from factors such as radiative cooling and warm air advec-

tions. The thickness of the inversion layer, influenced by the valley's unique orography, has been observed to vary, rarely exceeding 2200 m, with an average thickness around 1000 m. This characteristic plays a critical role in the valley's climatic conditions.

- **Inversion Strength and Duration:** The study reveals a stable pattern in inversion strength over the years with a Pearson correlation of 0.53 between inversion strength and duration. Occasional inversion strength outliers in the data suggest the influence of extraordinary meteorological events or anomalous environmental conditions, generating huge temperature gradients between the valley bottom (Prat Gran) and Engolasters.
- **Meteorological Variables Analysis:** The correlations between thermal inversions and meteorological variables are generally low and negative. The notable exception is the relative humidity at Prat Gran station, which shows a low but positive correlation. These findings highlight the complex interactions within the atmospheric system. High-pressure conditions, which are conducive to thermal inversions, are closely related to specific meteorological patterns. This underscores the importance of synoptic-scale dynamics in the formation and maintenance of inversion layers and also points to the significance of local processes in these phenomena.
- **Pollutant Analysis:** The study enhances the understanding of the impact of thermal inversions on air quality, particularly regarding NO_2 , PM_{10} , and O_3 . NO_2 concentrations significantly increase during inversion episodes, underscoring the role of atmospheric stability in the accumulation of this pollutant. While PM_{10} concentrations are influenced by external factors like Saharan dust, they also exhibit a complex relationship with thermal inversions. In contrast, O_3 levels demonstrate an inverse relationship with inversion episodes, likely due to interactions with other pollutants. Notably, all three pollutants have shown no correlation with the strength and duration of inversion events. In terms of meteorological data, NO_2 and PM_{10} display a stronger relationship with temperature, reflecting their accumulation during thermal inversion episodes. O_3 shows a closer correlation with wind, indicating its transport from other hotspots.

- **Low-Cost Sensor Analysis:** The effectiveness of tiny tags in capturing temperature variations has been a key focus, with their reliability varying based on location and altitude. The findings highlight the potential of these sensors in complementing traditional meteorological stations, especially in challenging terrains, though their limita-

tions in precision compared to more sophisticated equipment are noted.

In conclusion, this study sheds light on the intricate nature of thermal inversions in the Andorra Central Valley, revealing how geographical, meteorological, and anthropogenic factors collectively influence local climate dynamics. The exploration of low-cost sensors as viable tools for environmental monitoring opens up new possibilities for research and practical applications in meteorology and climatology. The insights gained from this study not only contribute to our understanding of thermal inversions but also underscore the need for integrated approaches in environmental monitoring and climate research.

ACKNOWLEDGMENTS

I would like to thank my university supervisor, Mireia Udina, for her unconditional support and for always having a smile, advising, and guiding me throughout the entire process. Also, my thanks go to the entire 'Andorra Recerca + Innovació' team, especially to Laura Trapero for acting as an external supervisor and for her guidance, and to Anna Albalat for her advice and the moments we shared. My gratitude extends to Roger Veciana i Rovira for introducing me to new insights about machine learning. Finally, I would like to express my heartfelt thanks to my family and friends for their unconditional support as well.

V. REFERENCES

- Beaufils, S., Wintertime mountain boundary layer in the central valley of andorra: temperature inversion and air quality, 2021.
- Bergot, T., An introduction to boundary layer meteorology, by roland b. stull, *La Météorologie*, 8(8), 89, doi: 10.4267/2042/53468, 1994.
- De Wekker, S., M. Kossmann, J. Knievel, L. Giovannini, E. Gutmann, and D. Zardi, Meteorological applications benefiting from an improved understanding of atmospheric exchange processes over mountains, *Atmosphere*, 9(10), 371, doi:10.3390/atmos9100371, 2018.
- Fochesatto, G. J., Methodology for determining multilayered temperature inversions, *Atmospheric Measurement Techniques*, 8(5), 2051–2060, doi:10.5194/amt-8-2051-2015, 2015.
- Giovannini, L., E. Ferrero, T. Karl, M. W. Rotach, C. Staquet, S. Trini Castelli, and D. Zardi, Atmospheric pollutant dispersion over complex terrain: Challenges and needs for improving air quality measurements and modelling, *Atmosphere*, 11(6), 646, doi:10.3390/atmos11060646, 2020.
- Grau, J. M. A., A., and J. Cuxart, Statistical characterization of the sea-breeze physical mechanisms through in-situ and satellite observations, *International Journal of Climatology*, 41(1), 17–30, doi:10.1002/joc.6606, 2020.
- Lageron, Y., and C. Staquet, Persistent inversion dynamics and wintertime PM10 air pollution in alpine valleys, *Atmospheric Environment*, 135, 92–108, doi: 10.1016/j.atmosenv.2016.03.045, 2016.
- Lu, Z. L., X., and L. Shen, Meteorology and climate influences on tropospheric ozone: A review of natural sources, chemistry, and transport patterns, *Current Pollution Reports*, 5(4), 238–260, doi:10.1007/s40726-019-00118-3, 2019.
- Mason, P. J., An introduction to boundary layer meteorology. by roland b. stull, reidel publishing co., dordrecht, 1988. pp. xii + 666. £64 (dfl 220), *Quarterly Journal of the Royal Meteorological Society*, 115(486), 423–423, doi: 10.1002/qj.49711548614, 1989.
- Pagès, P. N., M., and J. R. Miró, Measurement and modelling of temperature cold pools in the cerdanya valley (pyrenees), spain, *Meteorological Applications*, 24(2), 290–302, doi:10.1002/met.1630, 2017.
- Pepin, N., and D. Kidd, Spatial temperature variation in the eastern pyrenees, *Weather*, 61(11), 300–310, doi: 10.1256/wea.106.06, 2006.
- Russo, A., P. Sousa, R. Durão, A. Ramos, P. Salvador, C. Linares, J. Díaz, and R. Trigo, Saharan dust intrusions in the iberian peninsula: Predominant synoptic conditions, *Science of the Total Environment*, 717, 137,041, doi:10.1016/j.scitotenv.2020.137041, 2020.

VI. APPENDIX

Type	Name	Altitude (m)	Coordinates
Station	Prat Gran	1080	42.513000, 1.532400
Station	Engolasters	1638	42.516800, 1.565400
Tiny Tag	Panorama	1090	42.507882, 1.540934
Tiny Tag	Can Noguer	1280	42.511781, 1.552896
Tiny Tag	Coll de Jou	1295	42.515311, 1.548648
Tiny Tag	Borda Vilella	1360	42.512239, 1.555430
Tiny Tag	Bordes Engolasters	1530	42.512250, 1.563135
Tiny Tag	Coll Finestra	1660	42.497520, 1.537853
Tiny Tag	Braibal 1	1945	42.503278, 1.568944
Tiny Tag	Braibal 2	2165	42.504093, 1.579314

Table A.1: The 10 stations full dataset with their respective name, altitude, and decimal coordinates.

Station Name	Prat Gran Reference		Engolasters Reference	
	SD	MAD	SD	MAD
Borda Vilella	2.849879	2.852731	2.741248	2.441754
Can Nogueres	2.623297	2.294308	2.682111	2.814863
Coll Finestra	3.934283	4.438856	3.431865	2.278424
Coll de Jou	2.645086	2.402473	2.643443	2.696524
Hotel Panorama	2.583338	1.730073	3.441010	3.889384
Bordes Engolasters	2.740248	3.953492	2.485999	1.836393
Braibal 1	3.521835	5.627043	2.290110	2.096219
Braibal 2	3.575475	6.523003	2.280966	2.886720
Prat Gran	N/A	N/A	2.482517	4.056554
Engolasters	2.482517	4.056554	N/A	N/A

Table A.2: Summary of Precision Analysis for Temperature Data using Standard Deviation (SD) and Mean Absolute Deviation (MAD).

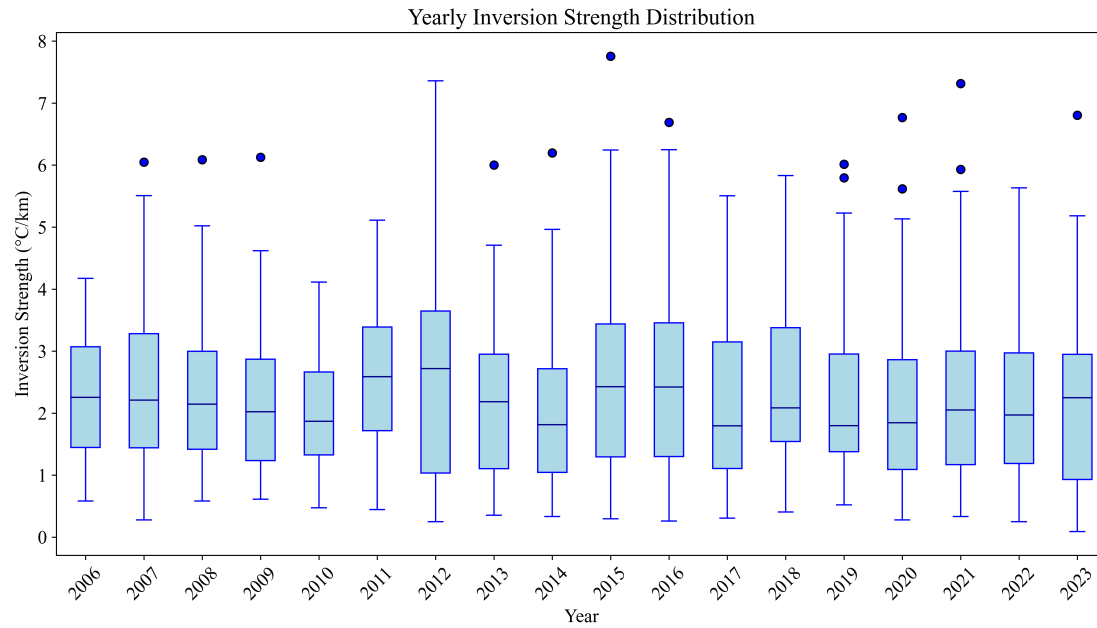


Figure A.1: Box plot with the Inversion Strength distribution over the years. Notice its homogeneity.

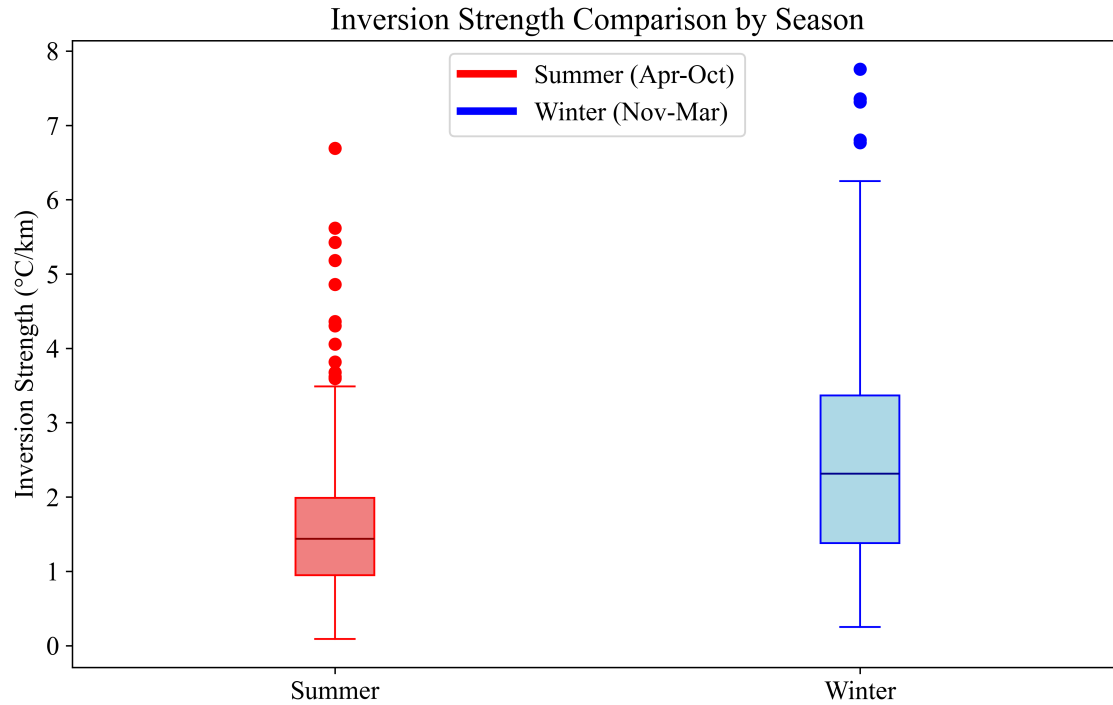


Figure A.2: Inversion Strength comparison between summer and winter seasons.

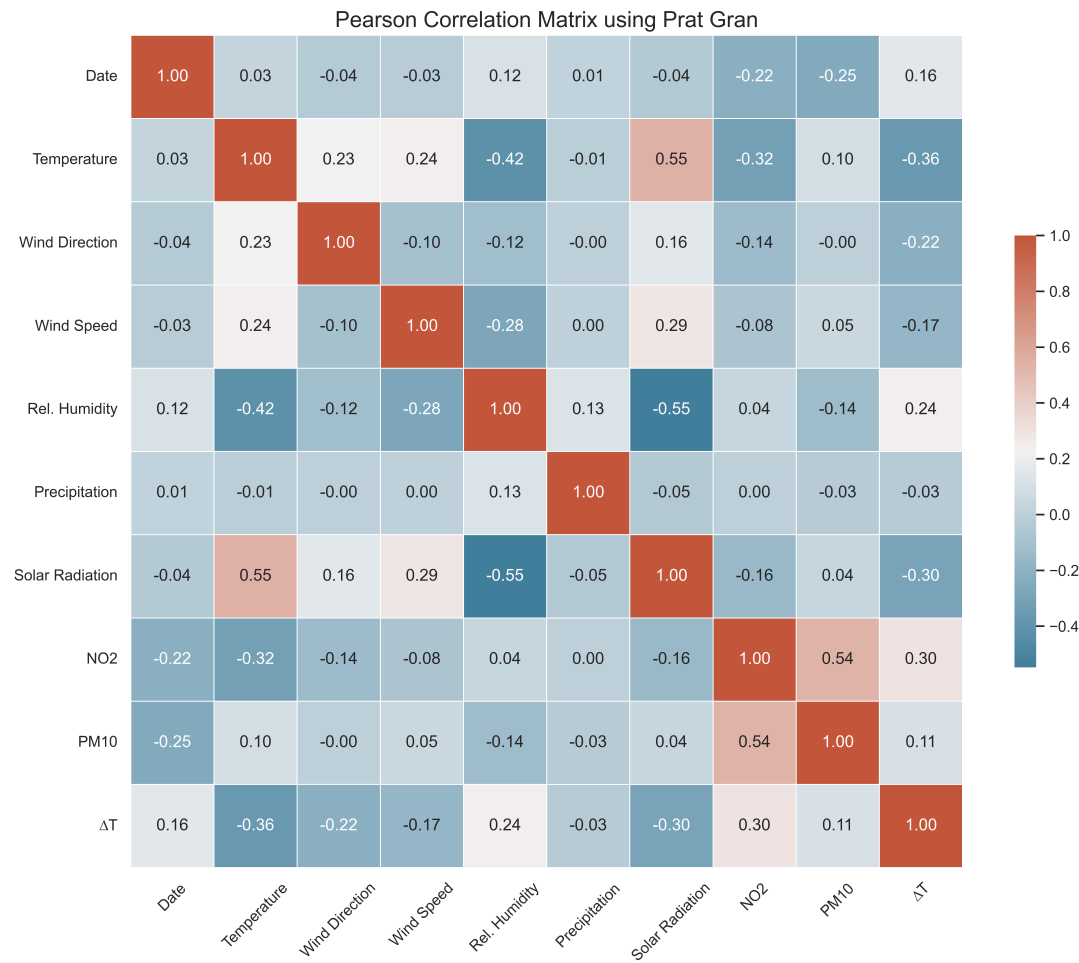


Figure A.3: Correlation Matrix calculated with all the available data in Prat Gran.

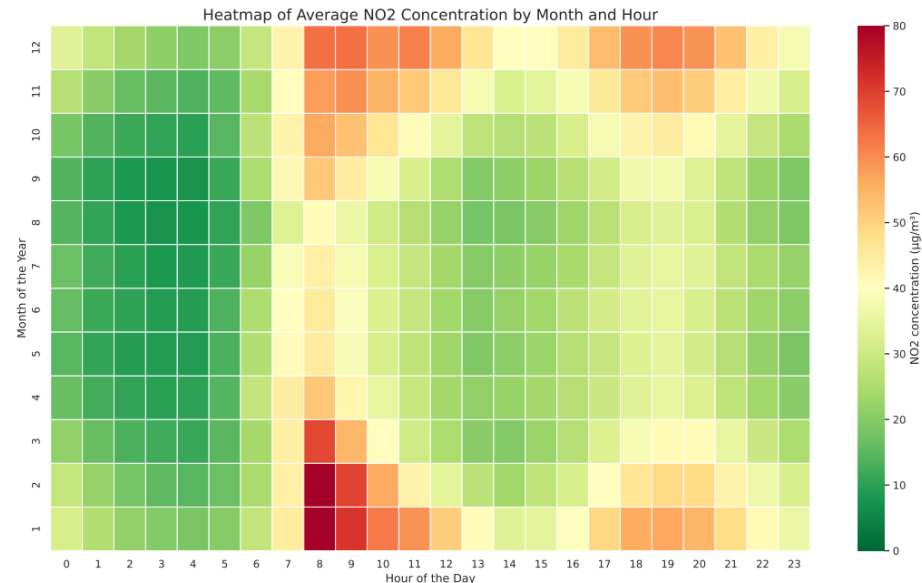


Figure A.4: Heatmap of average NO₂ concentration by month and hour.